Supporting information

A mesoporous carbon derived from 4,4'-dipyridyl iron as an efficient catalyst for oxygen reduction

Xiaohong Gao[a#], Xiaobao Li[b#], Qingqing Wang[a], Chenghang You[a*], Xinlong Tian[c*], Chongtai Wang[a], Yingjie Hua[a], Shijun Liao[d]

[a]The Key Laboratory of Electrochemical Energy Storage and Energy Conversion of Hainan Province School of Chemistry and Chemical Engineering, Hainan Normal University, Haikou 571158, China

[b]The Key Laboratory of Tropical Medicinal Plant Chemistry of Ministry of Education, School of Chemistry and Chemical Engineering, Hainan Normal University, Haikou 571158, China

[c]State Key Laboratory of Marine Resource Utilization in South China Sea, Hainan University, Haikou 570228, China

[d]The Key Laboratory of Fuel Cell Technology of Guangdong Province, School of Chemistry and Chemical Engineering, South China University of Technology, Guangzhou 510641, China

[#]These authors contribute equally.

[*]Corresponding authors

E-mail: youchh@163.com; tianxl@hainanu.edu.cn

Preparation of working electrodes

For electrochemical measurements, a glassy carbon electrode (GCE, Φ 5 mm) was used as the working electrode substrate. Before every measurement, the GCE was cleaned by ethanol in an ultrasonic bath, polished with α-Al_2O_3 slurry (50 nm) on a micro cloth, and rinsed with DI water.

For catalysts ink preparation, 5.0 mg catalyst and 1 mL Nafion ethanol solution (0.25 wt%) were thoroughly mixed under ultrasound for about 30 min. And then, 20 μL slurry was coated onto the GCE and dried naturally. The catalyst loading was calculated to be 0.5 mg cm^{-2}. For comparisons, a commercial Pt/C (20 wt%, Johnson Matthey Corp.) catalyst was also used for ORR.

Preparation of air electrode

For air electrode preparation, a Toray carbon paper (TGP-H-060) was used as the substrate. A diffusion layer was formed by painting the suspension of carbon black (XR-72R) and polytetrafluoroethylene (PTFE) onto one side of the carbon paper (the mass ratio of carbon black and PTFE is 3:2).

For catalyst layer fabrication, a catalyst ink was first prepared through the same procedure described in the working electrode preparation. The ink obtained was painted onto the other side of carbon paper and dried under an infrared lamp. The catalyst loading for NC-S900 is calculated to be 1.0 mg cm^{-2}. For comparisons, Pt/C was also used to fabricate an air electrode through the same procedures.

Characterization

The scanning electron microscopy (SEM) images were obtained on a JSM-7100F field emission scanning electron microscope (JEOL, Japan), with an acceleration voltage of 5 kV. The transmission electron microscopy (TEM) was operated on a JEM-2100 transmission electron microscope (JEOL, Japan) at an acceleration voltage of 200 kV. The X-ray photoelectron spectroscopy (XPS) was conducted on an ESCALAB 250 X-ray photoelectron spectrometer (Thermo-VG Scientific, USA). Catalysts' specific surface areas and pore size distribution were analysed by Brunauer-Emmett-Teller (BET) nitrogen adsorption-desorption at 77 K on a Tristar II 3020 gas adsorption analyzer (Micromeritics, USA).

Electrochemical measurements

Electrochemical measurements were carried out at room temperature by using a three-electrode glass cell on an Interface 1010B electrochemical workstation (Gamry, USA), coupled with a rotating ring-disk electrode (RRDE) system (PINE, USA). An Hg/HgO/NaOH (1M) and Pt wire was used as the reference and counter electrodes, respectively. All the potentials initially measured versus Hg/HgO/NaOH (1M) were converted to the ones versus reversible hydrogen electrode (RHE) by adding 0.92 V.

Before every measurement, the KOH solution (0.1 M) was saturated with O_2 (99.999%) or N_2 (99.999%) for at least 30 min. All the current densities were normalized to the GCE's geometric area (0.1964 cm^2).

The linear sweep voltammetry (LSV) measurements were conducted at a scan rate of 5 mV s^{-1} in an O_2 or N_2 saturated 0.1 M KOH solution.

The rotating ring-disk electrode (RRDE) measurements were conducted by using a glassy carbon disk with a Pt ring which was biased at 1.42 V (*vs.* RHE). The peroxide yields and the electron transfer number (n) per oxygen molecule were calculated based on the following equations[1]:

$$\eta = 200 I_r (\mathrm{N} I_d + I_r)^{-1}$$

$$n = 4 I_d (I_d + I_r \mathrm{N}^{-1})^{-1}$$

where I_r and I_d refer to the ring and disk currents, respectively, and N is the collection efficiency, which was confirmed to be 0.36 by the reduction of $K_3Fe(CN)_6$.

Battery tests

A home-made ZAB device was designed for the tests. A 6 M KOH solution containing 0.2 M zinc acetate was used as the electrolyte, and a zinc plate was used as the anode, respectively. The discharge-charge polarization curves were obtained by an Interface 1010B potentiostat (Gamry, USA). The full-discharge experiment was conducted by using galvanostatic technology on a BTS-3000 battery testing system (Newware, China) under the current density of 5 mA cm^{-2}.

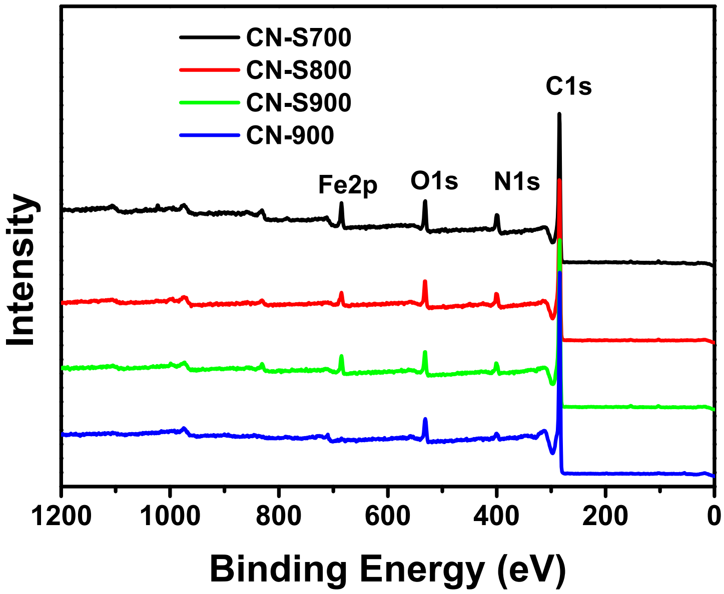

Fig. S1 XPS spectra of different catalysts

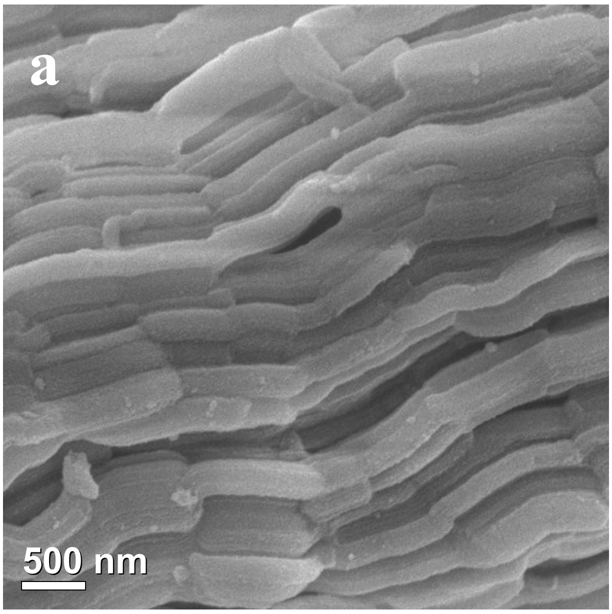

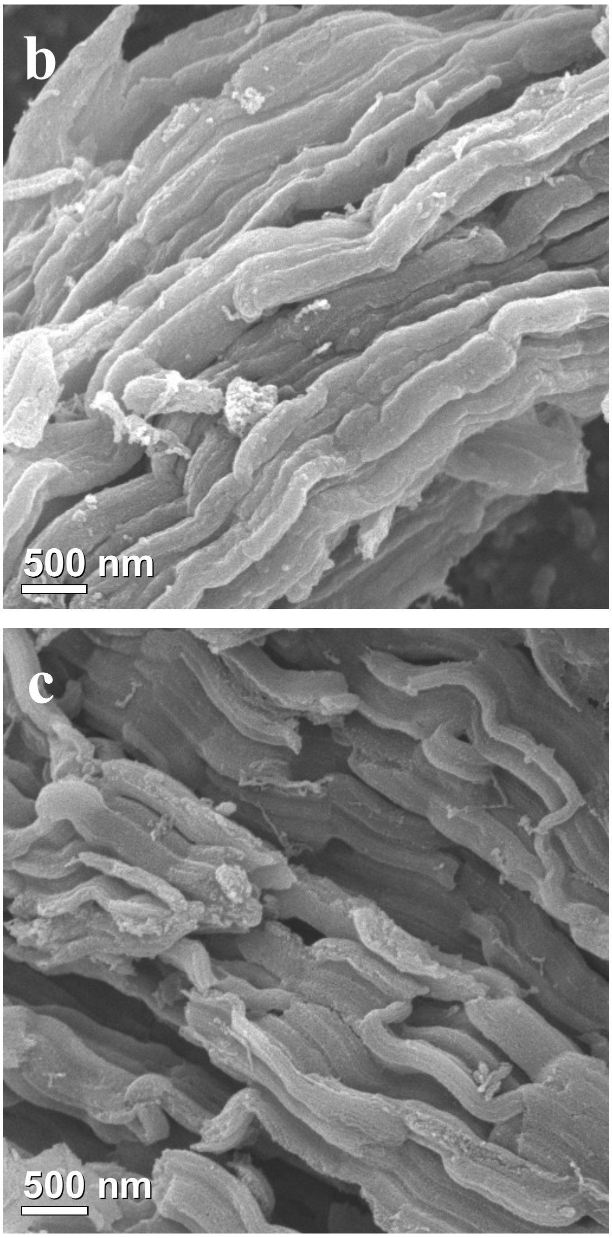
b
500 nm
c
500 nm

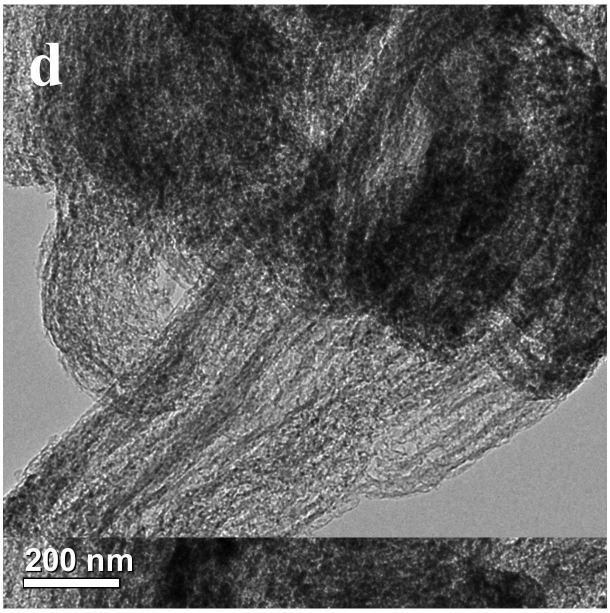

Fig. S2 SEM images: (a) dipy-Fe-SBA; (b) NC-S700; (c) NC-S800. (d) magnified TEM image of NC-S900

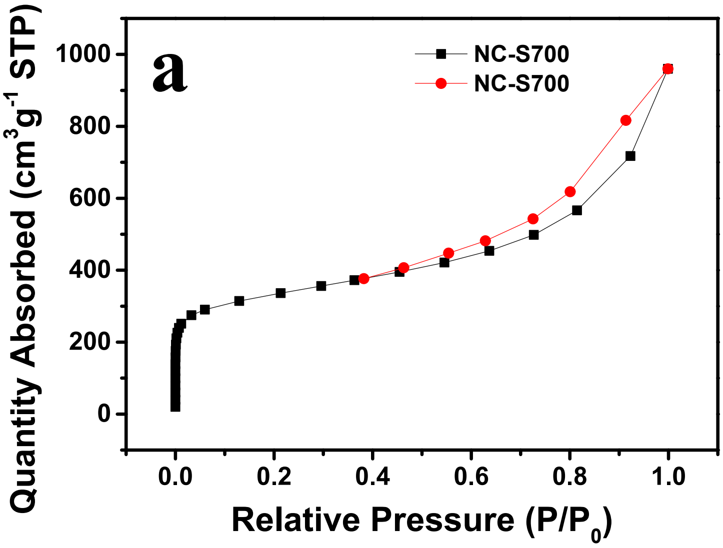

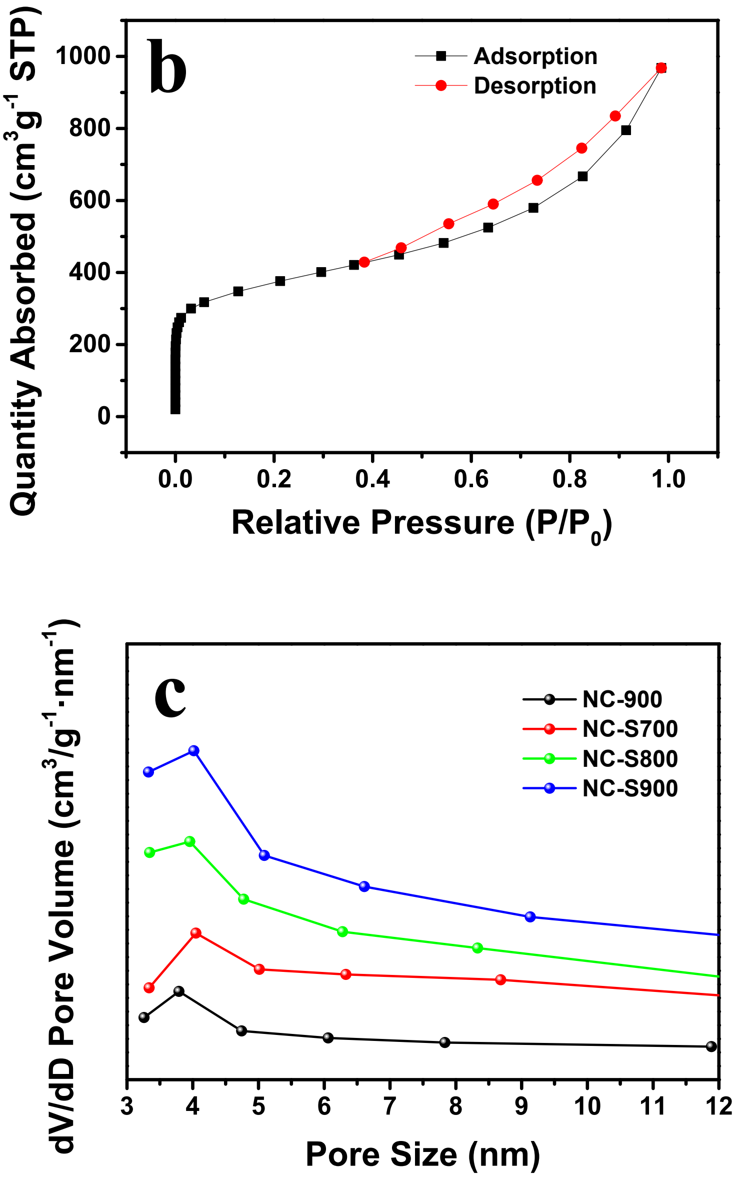

Fig. S3 N_2 adsorption-desorption isotherms: (a) NC-S700; (b) NC-S800; (c) Pore size distributions.

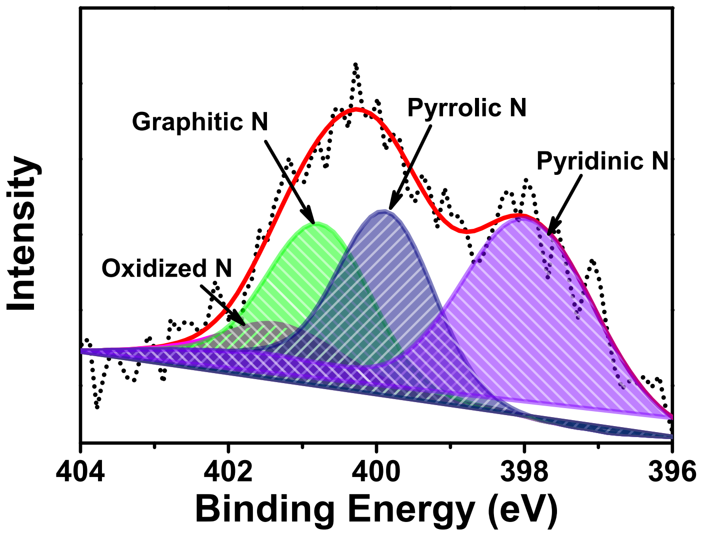

Fig. S4 High resolution N1s spectra of NC-900

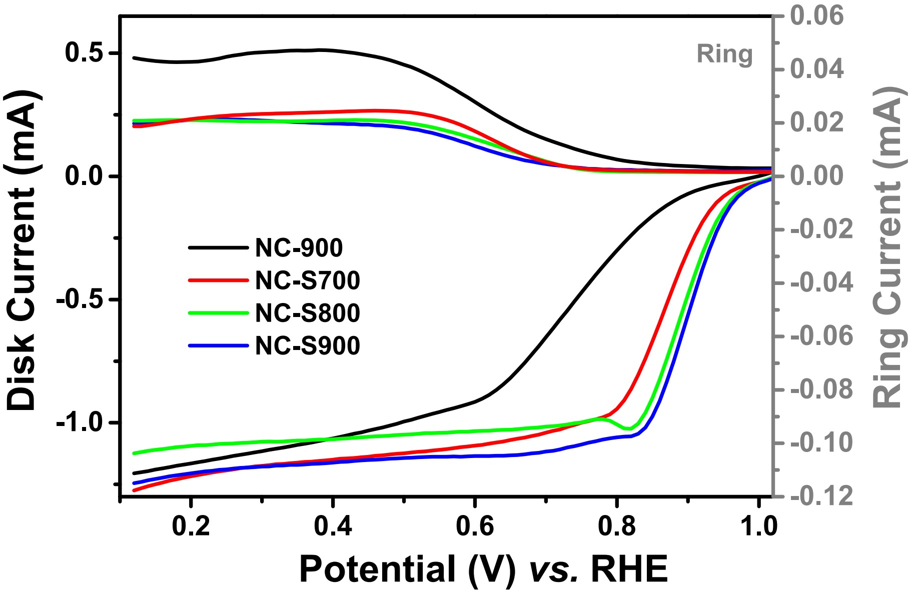

Fig. S5 RRDE curves of different catalsyts

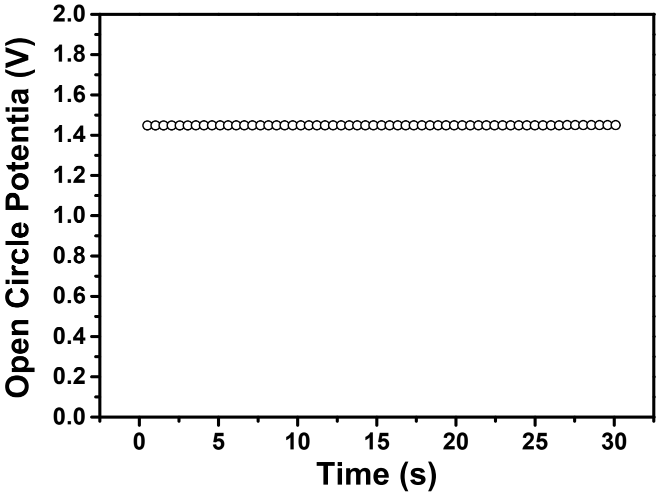

Fig. S6 open-circuit potential of ZAB based on NC-S900

Table S1 atomic compositions of various catalysts derived from XPS results

	NC-S700	NC-S800	NC-S900	NC-900
C	81.49	86.16	88.58	90.34
N	9.82	6.73	5.08	3.06
O	7.56	6.65	5.81	5.62
Fe	1.14	0.46	0.53	0.98

Table S2 relative content of different N species (%)

	oxidized	graphitic	pyrrolic	pyridinic
NC-S700	3.1	37.5	26.4	33.0
NC-S800	6.4	44.5	27.6	21.5
NC-S900	10.0	55.3	15.8	18.9
NC-900	5.5	23.3	27.0	44.3

Table S3 Half-wave potential ($E_{1/2}$) of recently reported ORR catalysts

No.	Catalyst	Electrolyte	$E_{1/2}$	Reference electrode	Reference
1	Co-Fe/NC-700	0.1 M KOH	0.854	RHE	[2]
2	1% Co-N-GDY	0.1 M KOH	0.81	RHE	[3]
3	SC-Fe	0.1 M KOH	0.869	RHE	[4]
4	Zn6Co	0.1 M NaOH	0.89	RHE	[5]
5	Fe SAs/N-C	0.1 M KOH	0.91	RHE	[6]
6	Co3O4@C/N-r-GO-10	0.1 M KOH	0.80	RHE	[7]
7	S-GNS/NiCo2S4	0.1 M KOH	0.88	RHE	[8]
8	Fe0.3Co0.7/NC	0.1 M KOH	0.88	RHE	[9]
9	FeSA-N-C	0.1 M KOH	0.891	RHE	[10]
10	FeNx/GM	0.1 M KOH	0.80	RHE	[11]
11	**NC-S900**	0.1 M KOH	**0.906**	RHE	**Our work**

Table S4 power density of ZABs recently reported

No.	Catalysts	Peak power density (mW cm^{-2})	Reference
1	Co3O4@Co/N-r-GO	172	[7]
2	Fe2Ni2N/Co@NCNT	300	[12]
3	FeZ-CNS-900	168	[13]
4	Co-SAs@NC	105.3	[14]
5	CCOPTDP–FeNi–SiO2	112.8	[15]
6	FeCo@C MS	86.9	[16]
7	CoFe/N-GCT	203	[17]
8	S-GNS/NiCo2S4	216.3	[8]
9	Fe/N/S-CNTs	111	[18]
10	0.1-Co-NHCs	239.8	[19]
11	**NC-S900**	**196.3**	**Our work**

References

1. J. Wang, G. Wang, S. Miao, X. Jiang, J. Li and X. Bao, *Carbon*, 2014, **75**, 381-389.
2. S. L. Zhang, B. Y. Guan and X. W. Lou, *Small*, 2019, **15**, 1805324.
3. X. Wang, Z. Yang, W. Si, X. Shen, X. Li, R. Li, Q. Lv, N. Wang and C. Huang, *Carbon*, 2019, **147**, 9-18.
4. J. Xie, B.-Q. Li, H.-J. Peng, Y.-W. Song, J.-X. Li, Z.-W. Zhang and Q. Zhang, *Angew. Chem. Int. Edit.*, 2019, **58**, 4963-4967.
5. Y. Xiong, Y. Yang, F. J. DiSalvo and H. D. Abruna, *J Am Chem Soc*, 2019, **141**, 10744-10750.

6. Z. Yang, Y. Wang, M. Zhu, Z. Li, W. Chen, W. Wei, T. Yuan, Y. Qu, Q. Xu, C. Zhao, X. Wang, P. Li, Y. Li, Y. Wu and Y. Li, *Acs Catal*, 2019, **9**, 2158-2163.

7. L. Zhang, X. Yang, R. Cai, C. Chen, Y. Xia, H. Zhang, D. Yang and X. Yao, *Nanoscale*, 2019, **11**, 826-832.

8. W. Liu, J. Zhang, Z. Bai, G. Jiang, M. Li, K. Feng, L. Yang, Y. Ding, T. Yu, Z. Chen and A. Yu, *Adv Funct Mater*, 2018, **28**, 1706675.

9. B. Y. Guan, Y. Lu, Y. Wang, M. Wu and X. W. D. Lou, *Adv Funct Mater*, 2018, **28**, 1706738.

10. L. Jiao, G. Wan, R. Zhang, H. Zhou, S.-H. Yu and H.-L. Jiang, *Angew Chem Int Edit*, 2018, **130**, 8661-8665.

11. X. Fu, N. Li, B. Ren, G. Jiang, Y. Liu, F. M. Hassan, D. Su, J. Zhu, L. Yang, Z. Bai, Z. P. Cano, A. Yu and Z. Chen, *Adv. Energ. Mater.*, 2019, **9**, 1970031.

12. M. Wu, G. Zhang, J. Qiao, N. Chen, W. Chen and S. Sun, *Nano Energy*, 2019, **61**, 86-95.

13. G. Li, L. Pei, Y. Wu, B. Zhu, Q. Hu, H. Yang, Q. Zhang, J. Liu and C. He, *J. Mater. Chem. A*, 2019, **7**, 11223-11233.

14. X. Han, X. Ling, Y. Wang, T. Ma, C. Zhong, W. Hu and Y. Deng, *Angew. Chem. Int. Edit.*, 2019, **58**, 5359-5364.

15. J. Guo, T. Li, Q. Wang, N. Zhang, Y. Cheng and Z. Xiang, *Nanoscale*, 2019, **11**, 211-218.

16. Y. Xu, B. Chen, J. Nie and G. Ma, *Nanoscale*, 2018, **10**, 17021-17029.

17. X. Liu, L. Wang, P. Yu, C. Tian, F. Sun, J. Ma, W. Li and H. Fu, *Angew. Chem.*

Int. Edit., 2018, **57**, 16166-16170.

18. H. Jin, H. Zhou, W. Li, Z. Wang, J. Yang, Y. Xiong, D. He, L. Chen and S. Mu, *J. Mater. Chem. A*, 2018, **6**, 20093-20099.

19. S. Chen, J. Cheng, L. Ma, S. Zhou, X. Xu, C. Zhi, W. Zhang, L. Zhi and J. A. Zapien, *Nanoscale*, 2018, **10**, 10412-10419.